1 Introduction to Multiphase Fluid Dynamics

1.1 Multiphase Flow and Book Scope

The term *multiphase flow* denotes fluid dynamics with two or three phases, where each phase can be a solid, liquid, or gas. If one of these phases is distributed in small, unattached elements (such as particles, drops, or bubbles), this phase is a dispersed matter and the combination of phases becomes a "dispersed" multiphase flow, which distinguishes it from a free-surface multiphase flow (such as wind over water). The four primary combinations for the dispersed two-phase flows shown in Figure 1.1 include:

(1) Solid particles in a gas
(2) Liquid drops in a gas
(3) Solid particles in a liquid
(4) Gas bubbles in a liquid

Three-phase flow is an extension of two-phase flow and consists of two primary combination sets: liquid drops and solid particles in a gas (e.g., spray and soot in a combustion chamber) or gas bubbles and solid particles in a liquid (e.g., bubbles and sand in the ocean). Herein, we will use the term "particle" to represent either a solid particle, a liquid drop, or a gas bubble.

This book focuses on flow regimes for which the dynamics of the particles (solid particles, drops, or bubbles) is primarily controlled by the surrounding fluid. Such conditions can include a complex array of particle dynamics phenomena such as acceleration by drag, gravitational settling, turbulent dispersion, collisions, coalescence, breakup, etc. The presence of a large concentration of particles can also lead to coupling effects between the phases that can modify the flow fields of the surrounding fluid, especially when the surrounding flow is turbulent.

Heat and mass transfer as well as dense flows are not a focus of this text but can be important for many multiphase flows. Multiphase heat transfer can stem from conduction, convection, and/or radiation, while mass transfer can be associated with evaporation, condensation, and/or combustion. Dense flow can include granular flow and other regimes where particle motion is dominated by interaction with other particles (instead of by interaction with the surrounding flow). Readers with an interest in heat and mass transfer and/or dense flows should consider the texts recommended in the preface.

In general, analysis of multiphase flow requires careful consideration of the physics, governing equations, models, and numerical schemes that are key to the

https://doi.org/10.1017/9781139028806.002 Published online by Cambridge University Press

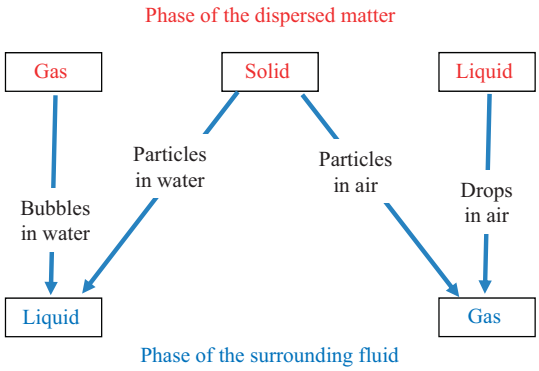

Figure 1.1 Various combinations for the dispersed phase and the surrounding fluid phase for two-phase flows.

characteristics and flow regimes of interest. These aspects are discussed in Chapters 2–11. The first eight chapters include homework sets (e.g., §1.6 for this chapter), and the last three chapters include reference material.

The rest of Chapter 1 introduces and identifies systems with dispersed multiphase flow and then provides key nomenclature, reference frames, and assumptions. The following section (§1.2, where § indicates a section of the text) discusses several engineered and natural systems with respect to multiphase flow. The remaining sections of this chapter set forth key terminology and assumptions for dispersed multiphase flow (§1.3), the key velocity reference frames used for multiphase flow (§1.4), and the assumption of continuum conditions (§1.5).

1.2 Multiphase Flow in Engineered and Natural Systems

Particle-laden flows are important to a wide variety of engineered and natural systems. Engineered systems include aerospace, atmospheric, biological, chemical, civil, mechanical, and nuclear applications. Examples of two-phase flows are listed in Table 1.1a for engineered systems and in Table 1.1b for natural systems. The flows can also be grouped in the following three system types:

(1) Energy and propulsion systems
(2) Manufacturing, processing, and transport systems
(3) Environmental and biological systems

These three groups are considered in the following subsections in terms of the key multiphase flow issues and physics.

1.2.1 Multiphase Flow in Energy and Propulsion Systems

Energy systems often include multiphase flow. For example, wind turbine blades must be designed to withstand particle erosion as well as ice accretion (Figure 1.2). Both

https://doi.org/10.1017/9781139028806.002 Published online by Cambridge University Press

Table 1.1 Two-phase flow combinations for (a) engineered systems and (b) natural systems.

(a)

Two-phase flows	Engineering applications
Solid particles in a gas	Solid rockets, fluidized beds, particle separators, clean rooms
Liquid droplets in a gas	Fuel sprays, printing, coating and plasma sprays, cooling, aerosols
Solid particles in a liquid	Chemical slurries, liquid filters, sedimentation, fluidized beds
Gas bubbles in a liquid	Naval vessels, bubble columns, molten metal baths, boilers

(b)

Two-phase flows	Natural systems
Solid particles in a gas	Snow, sand, volcanic ash, pollen in air
Liquid droplets in a gas	Rain, drizzle, fog, ocean spray
Solid particles in a liquid	Sand or sediment flowing in a river
Gas bubbles in a liquid	Underwater plumes, cresting waves

Figure 1.2 Icing on a wind turbine blade caused by impact of freezing rain or drizzle (Larrsen, 2021).

icing and erosion are complex multiphase flows that involve particle trajectories that are influenced by the local aerodynamics and the impact physics. Another energy system that includes multiphase flow is energy production from combustion, whose products can include soot particles, which are ideally filtered from the exhaust gases. For coal combustion, particle filtering of soot particles and ash for the exhaust are important, as indicated by particulate control devices (see the right-hand side of Figure 1.3). A common approach for such filtering is to employ cyclone filters

https://doi.org/10.1017/9781139028806.002 Published online by Cambridge University Press

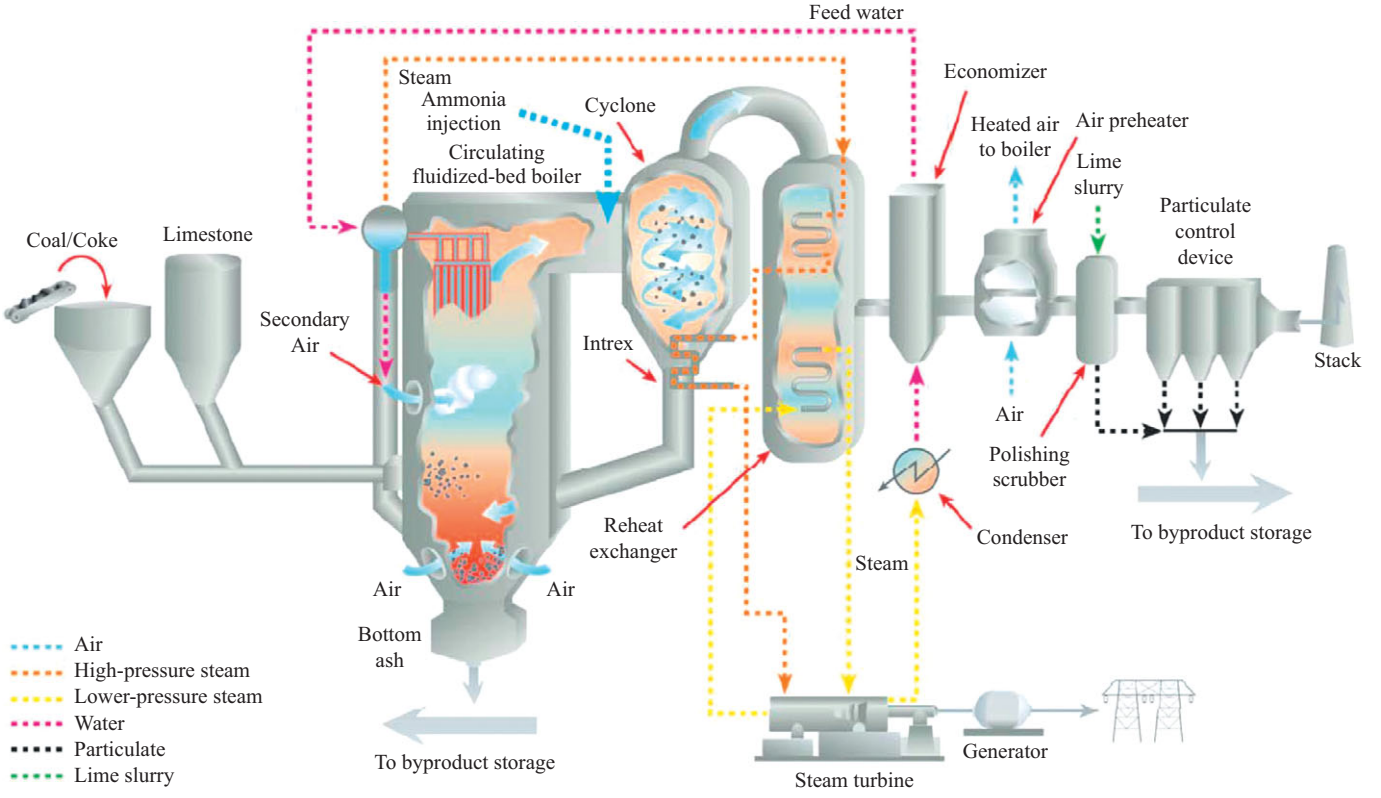

Figure 1.3 Schematic of a coal combustion plant with circulating fluidized bed and downstream particle separation using return channels, cyclones, and eventually cloth filters to help ensure a clean exhaust to atmosphere. Photograph (2020) Alyeska Pipeline Service Company (APSC), used with permission.

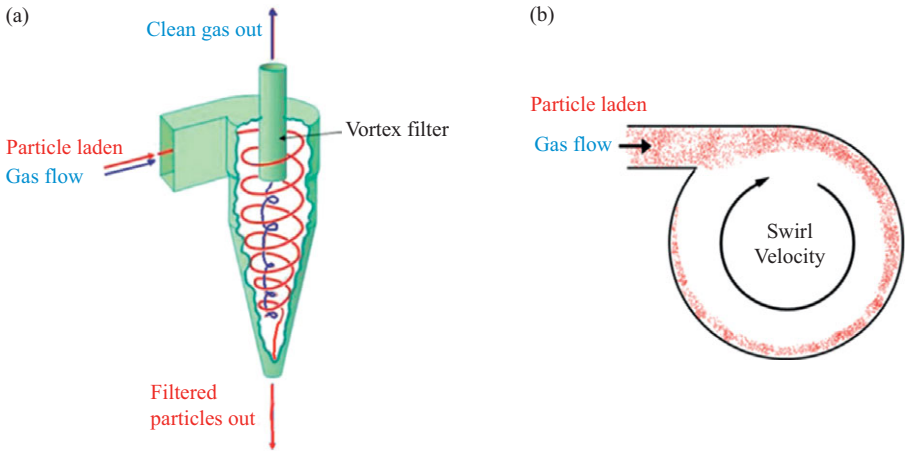

Figure 1.4 Schematic of a dust collector based on a cyclone separator used to allow downward gravitational collection of particles while cleaner gas tends to exhaust upward as clean (particle-free): (a) overall view; and (b) cross-sectional view showing particles centrifuged outward by swirl velocity.

(Figure 1.4), which use centrifugal and gravity forces to achieve separation of the particles from the gas stream. Multiphase flow for these coal-fired plants is also critical for the fuel feed and fluidized bed regions (see the left-hand side of Figure 1.3).

Air-breathing power and propulsion systems also generally involve multiphase flow. For example, a turbojet engine can have particles in the inlet, the combustor, and the exhaust, as shown in Figure 1.5a. Particulate matter from the entering flow can lead to blade damage or problematic blade accretion in the high-speed compressor section. To avoid this, a centrifugal separator can be used to cyclone out the particles. Following the compressor, the combustor also includes multiphase flow stemming from the spray nozzles used to produce fuel droplets. The combustion process is enhanced when the droplets are small (e.g., less than 40 μm in diameter), which can be achieved with rapid drop breakup using a pressurized swirl nozzle (Figure 1.5b). When these drops are uniformly distributed in the combustor, which can be achieved with mixing by turbulent dispersion, the combustion efficiency is higher and the soot is lower, thus minimizing environmental impact.

Multiphase flow can also be important for energy storage systems that support intermittent renewable energy (such as wind and solar energy). For example, compressed air energy storage can be made highly efficient if the process is made nearly isothermal (Qin et al., 2014). This can be achieved by spraying droplets (with a high surface area for enhanced heat transfer) during compression for energy storage (Figure 1.6) and during expansion for energy regeneration.

Another energy-producing system that promotes grid decarbonization and involves multiphase flow is a nuclear power plant. These systems generally use the heat from the nuclear reactor to convert water into steam to drive power-generating turbines. The boiling initially creates a bubbly flow (whose volume is mostly composed of liquid)

https://doi.org/10.1017/9781139028806.002 Published online by Cambridge University Press

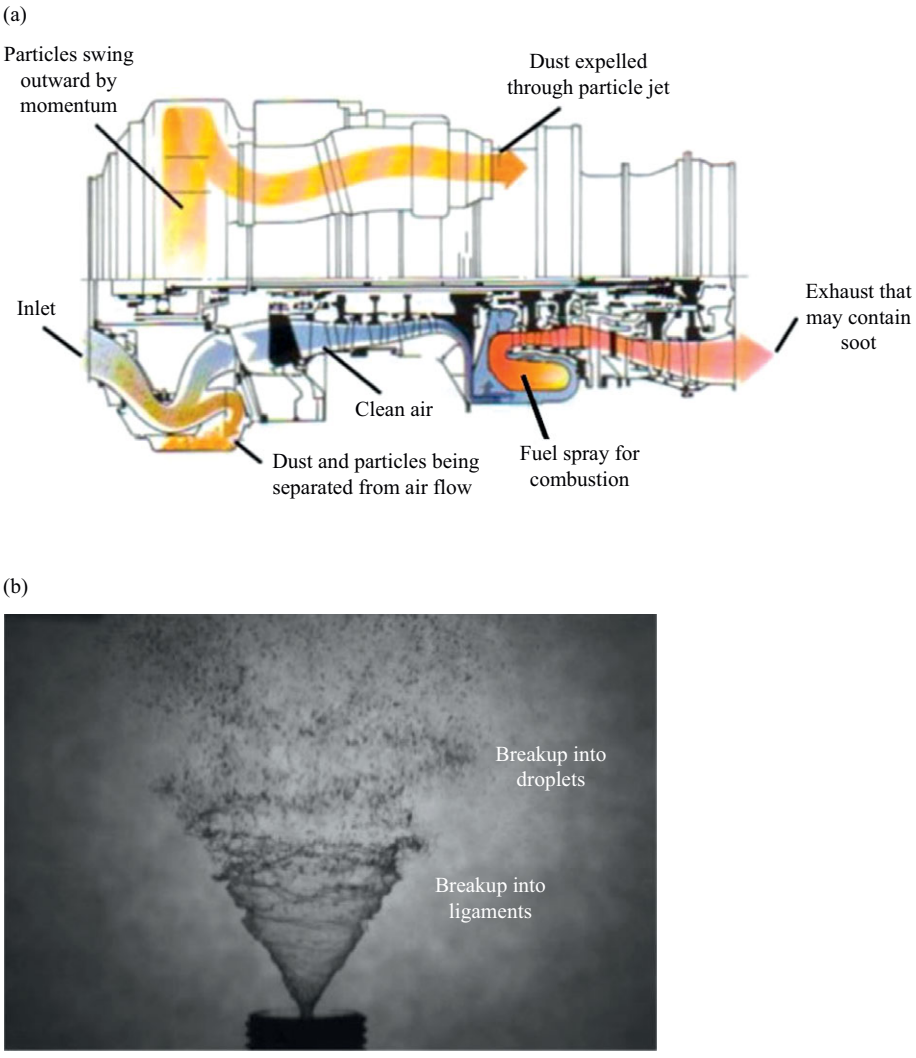

Figure 1.5 (a) Multiphase aspects of an air-breathing engine that includes a fuel spray in the combustor (Yoon, 2001); and (b) close-up of pressure swirl spray where instabilities transition the conically spreading liquid sheet to ligaments and then into droplets, which can spread through turbulence (Prakash et al., 2014).

and eventually creates a steam flow (a gas vapor flow with drops). This process is associated with high heat and mass transfer rates as well as nonuniform turbulent flow and interfacial dynamics governed by surface tension, all of which are important but cannot be easily predicted. As such, high-fidelity multiphase flow experiments and simulations are critical to effective and efficient plant design.

Multiphase flow is also important to solid rocket propulsion since the combustion processes involve particulate burning. The solid propellant starts off as a packed

https://doi.org/10.1017/9781139028806.002 Published online by Cambridge University Press

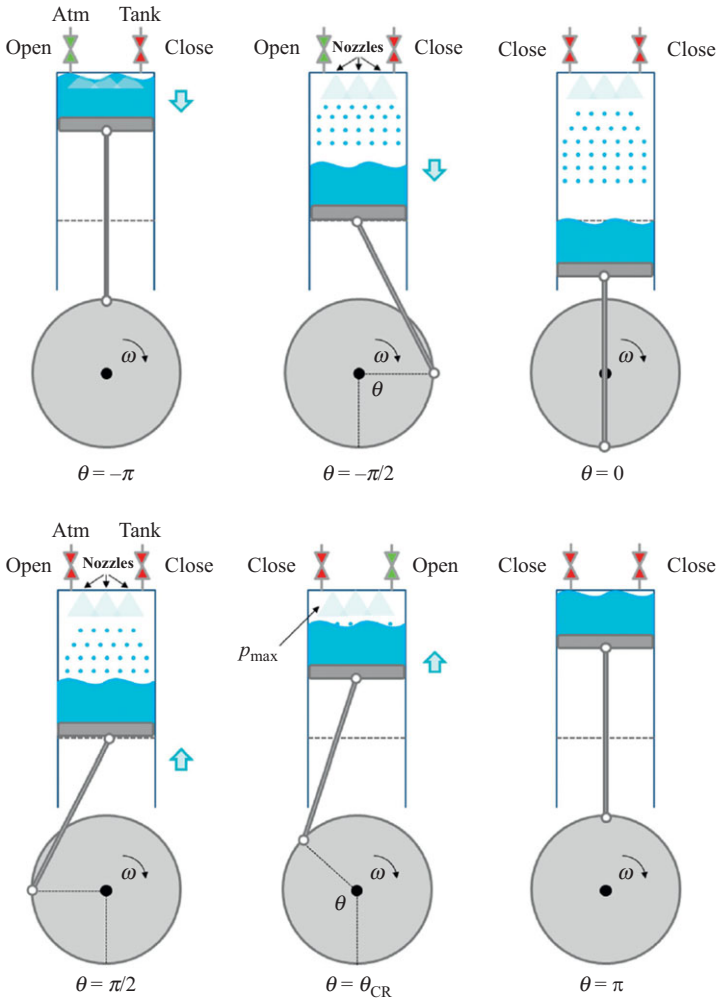

Figure 1.6 Injection of spray droplets for a liquid piston compression system to achieve near-isothermal conditions for compressed air energy storage (Qin et al., 2014).

mixture of powdered fuels and oxidizers integrated with a binder (Figure 1.7a). This mixture can include aluminum particles to achieve very high reaction temperatures (1,500–3,500 K). As shown in Figure 1.7b, many of the particles do not combust immediately and instead break off as the binder around them burns away. As these particles move downstream, they mostly melt, evaporate, and generally combust, yielding high-pressure gas products before they reach the end of the combustion chamber. However, any particles that are still molten are problematic since they can impact and accrete around the nozzle throat (leading to a slag buildup that can cause choking) or can impact the nozzle surface with high-velocity impacts (leading to ablation).

https://doi.org/10.1017/9781139028806.002 Published online by Cambridge University Press

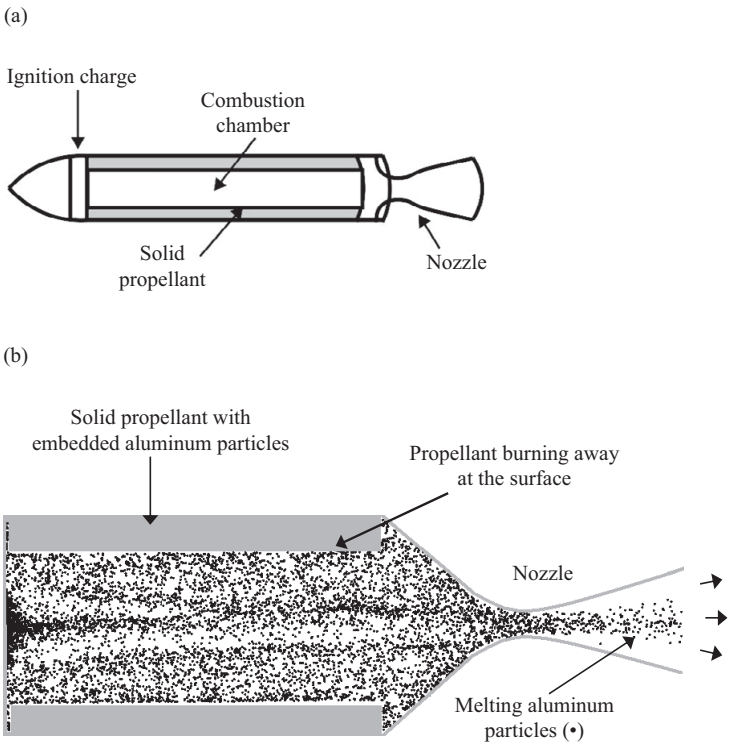

Figure 1.7 (a) Schematic of a solid propellant rocket that uses a combustion chamber to create high-enthalpy gas for propulsion. (b) Particles distributed in the combustion chamber that are released from solid propellant walls as the surface burns away and generally combust as they move downstream, that is, to the right (Najjar, 2005).

1.2.2 Multiphase Flow in Manufacturing, Processing, and Transport Systems

Manufacturing processes often involves multiphase flows. For example, coatings on surfaces are often applied using spray systems that are designed to generate droplets that are small enough to ensure a smooth finish, yet large enough to avoid being carried away from the target zone by surrounding air crossflows.

To create extremely durable metal coatings, one may employ plasma spraying (Figure 1.8a). In this type of coating process, metal powder is injected into a high-temperature plasma arc jet, created by a high-voltage difference (Figure 1.8b). The particles melt and then impinge on the target surface, where they rapidly crystallize to form a single-crystal metallic coating. This coating can survive hostile environments (needed for gas turbine blades) and can have extremely long usage without wear (needed for medical implants). The coating performance is strongly related to the multiphase flow aspects, such that the combination of the flow conditions and temperatures as well as the material and size of the particles are carefully controlled.

https://doi.org/10.1017/9781139028806.002 Published online by Cambridge University Press

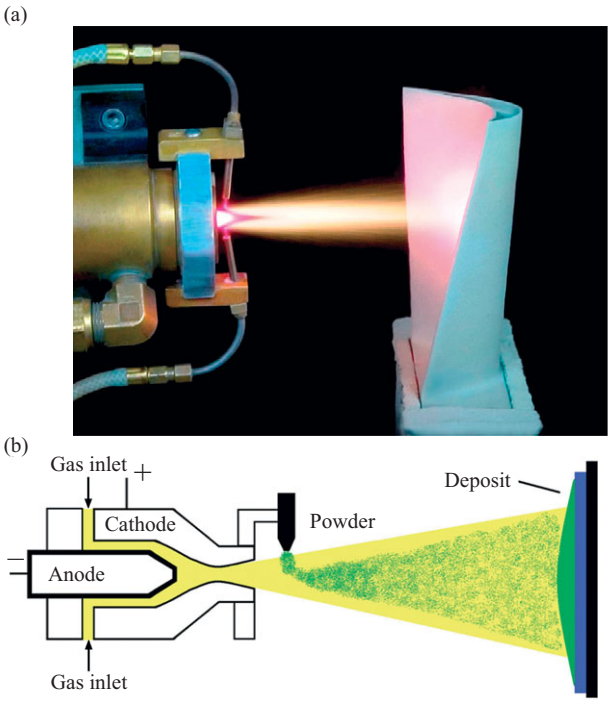

Figure 1.8 Plasma sprays: (a) applied to a turbine blade (JTJ, 2013); and (b) schematic of a spray system where metal particles are entrained into gas field (yellow) that exits as high-temperature plasma causing the particles to melt (or even evaporate) before they deposit on the target surface, where they create a highly durable metallic coating based on single-crystal growth.

Another multiphase manufacturing process is the production of powders. Many foods, detergents, and pharmaceuticals require their powders to be very fine with high consistency of size and shape. These characteristics can be achieved with an industrial spray dryer (Figure 1.9a), where liquid sprays are converted to powders through solidification. For this process, a warm liquid emulsion feed is sprayed downward into a large chamber, where the droplets cool and solidify as they fall to create a fine powder (Figure 1.9b). To create micropowders (Figure 1.9c), some dryers apply high-frequency vibrating spray nozzles to create extremely small droplets.

Multiphase processing is used in the production of many chemical products to promote chemical reactions and mixing. For example, liquid chemical reactors often employ bubble columns and recirculating reactors (Figure 1.10) to increase interfacial surface area and thus the corresponding reaction and mass transfer rates between the phases. Other examples of multiphase reactors include bio-oxygenation, distillation, and chromatography columns as well as fermentation bioreactors.

Multiphase flow can also be used to transport solid particles in pipe systems. This can be achieved by air-driven pneumatic conveyors (generally used for low particle concentrations at high speeds) or by liquid-driven slurries (generally used for high particle concentrations at low speeds). Generally, the flows are turbulent, making the

https://doi.org/10.1017/9781139028806.002 Published online by Cambridge University Press

(a)

(b)

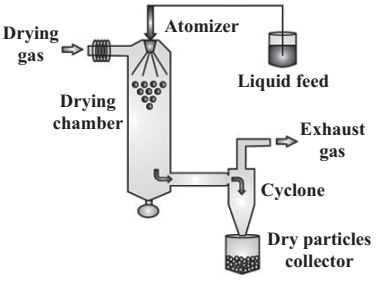

(c)

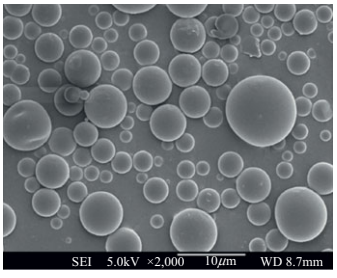

Figure 1.9 Spray dryers used to create powders: (a) a large-scale industrial spray dryer facility (GEA, 2020); (b) schematic of a process that includes an atomizer to create powder in a dry gas and the resulting mixture is fed to a cyclone filter to extract the product downward while clean air exhausts upward (Sosnick and Seremeta, 2015); and (c) microparticles (ranging from 2–10 μm in diameter) generated by a vibrating mesh spray imaged with a scanning electron microscope (Lee et al., 2011).

interactions quite complex. In such cases, understanding the particle trajectory dynamics and their interaction with the driving flow is important to help reduce pipe pressure losses (to minimize energy requirements) while ensuring particles are fully suspended within the flow (to maximize transport efficiency).

Transporting liquids with pumps can also involve multiphase flow, since the impellers can yield problematic cavitation. This occurs when the blade speeds are high enough to cause the local liquid pressure to drop below the vapor pressure. For example, steam bubbles are formed out of water at low enough pressure. These vapor bubbles can reduce impeller efficiency since they can lead to flow separation. In addition, the vapor bubbles entering high-pressure regions will rapidly collapse, and this can lead to significant blade damage (surface pitting) if this occurs near the

https://doi.org/10.1017/9781139028806.002 Published online by Cambridge University Press

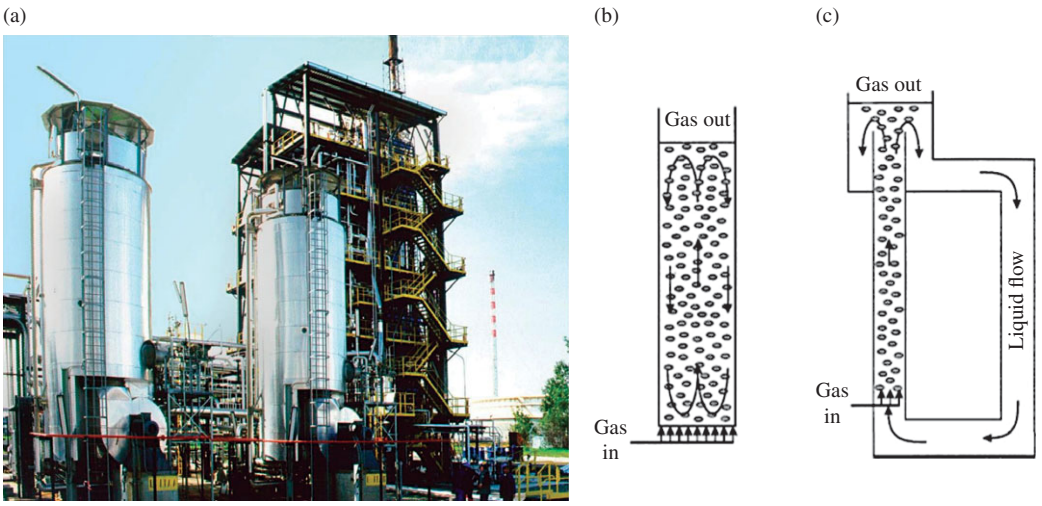

Figure 1.10 Bubble column reactors: (a) an industrial single-column reactor (P. M. Raimundo, ENI, IFP Energies Nouvelles, Etablissement de Lyon, France, personal communication, 2020); (b) schematic of a single-column reactor; and (c) schematic of a recirculating airlift reactor (Mudde and Saito, 2001).

surface. Cavitation can be similarly problematic for propellers of ships and underwater vehicles in terms of propulsive efficiency and blade damage.

However, multiphase flow can be beneficial for transporting liquids in turbulent flows when used for drag reduction. In particular, microbubbles (about 10–100 μm in diameter) and long-chain polymers (with molecular weight greater than 10^5) in turbulent boundary layers have both been found to significantly reduce the shear drag by as much as 75% (Figure 1.11a). In both cases, the injected microbubbles or polymers reduce the near-wall turbulent momentum mixing through dissipative interactions with the boundary-layer vortices. These microbubbles and polymers are active when their response time scales (drag based for the bubbles and coil based for the polymers) are similar to the turbulent microscales (Pal et al., 1988). The polymer approach has been most successful for engineered systems. For example, polymers injected into the Alaskan oil pipeline (Figure 1.11a) allow oil flow rates to be increased by as much as 50% without increasing the pumping power. Polymers can also be mixed with water to reduce liquid skin friction in fire hoses, thereby increasing nozzle water velocity and the resulting distances and heights that can be reached by the exiting water stream. Interestingly, the bubble approach for drag reduction is observed in nature. In particular, penguins have the ability to collect a gas layer under the feathers before entering the water and then later release this gas underwater in the form of microbubbles (Figure 1.12a). This significantly reduces their fluid dynamic skin friction drag, allowing them to make a burst of speed to catch prey or to jump out of the water. Marine vessel designers are investigating injection of microbubbles along their hulls to help reduce fuel consumption using this bio-inspired concept (Figure 1.12b).

https://doi.org/10.1017/9781139028806.002 Published online by Cambridge University Press

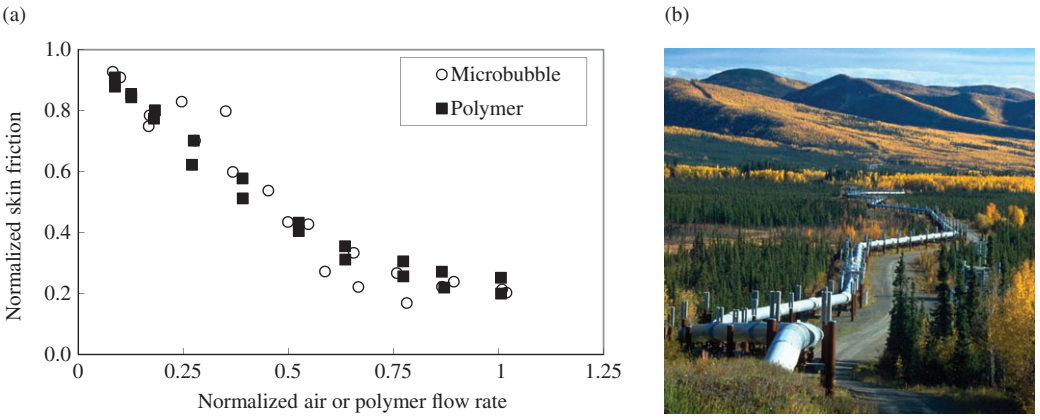

Figure 1.11 Turbulent drag reduction with multiphase flow: (a) measured in a boundary layer (Pal et al., 1988) based on normalized concentrations for microbubbles (relative to 30% by volume loading) or long-chain polymers (relative to 0.5% by mass loading); and (b) the Trans-Alaska Pipeline, which uses polymers that increased the pipe flow from 1.44 billion barrels per day to 2.14 billion barrels per day (Nielsen et al., 1999).

Microbubbles can also be used for specialized manufacturing with a process called *sonoluminescence*, in which sound is converted to light (Figure 1.13). In particular, micron-scaled bubbles can be subjected to strong, highly focused acoustic oscillations at their natural frequency to generate rapid and large oscillations in bubble diameter. The contraction portion of these oscillations can lead to high gas compression with the extreme pressures and temperatures such that the gas inside becomes a plasma (Figure 1.14a). The emitted light when this gas turns into a plasma can even be seen with the unaided eye (Figure 1.14b). The increased local temperatures can allow the production of protein microspheres (Figure 1.14c), whereby a shell of protein is formed over the microbubble through cross-linking.

1.2.3 Multiphase Flow in Biomedical and Environmental Systems

Multiphase flow is also critical to a wide range of biomedical systems and environmental systems. In some case, particles are intentionally introduced by medical procedures for the purpose of diagnostic imaging or drug delivery. For example, microbubbles can be injected into the bloodstream and subjected to sonic waves so that they oscillate and create acoustic signals that can be used for diagnostic purposes. Differences in these acoustic signals can be used to identify regions of good versus bad blood flow circulation, and even identify tumors (Figure 1.13). Blood itself is also multiphase compilation of liquids (plasma) and soft particles (platelets, red blood cells, white blood cells, lymphocytes, etc.). This can create complex rheology in the smaller vessels. In addition, blood can also include small calcium particles, which can problematically deposit and build up on vessel walls. The resulting accretion is called plaque and can cause a narrowing or blockage of the blood vessels, which leads to poor blood circulation,

https://doi.org/10.1017/9781139028806.002 Published online by Cambridge University Press

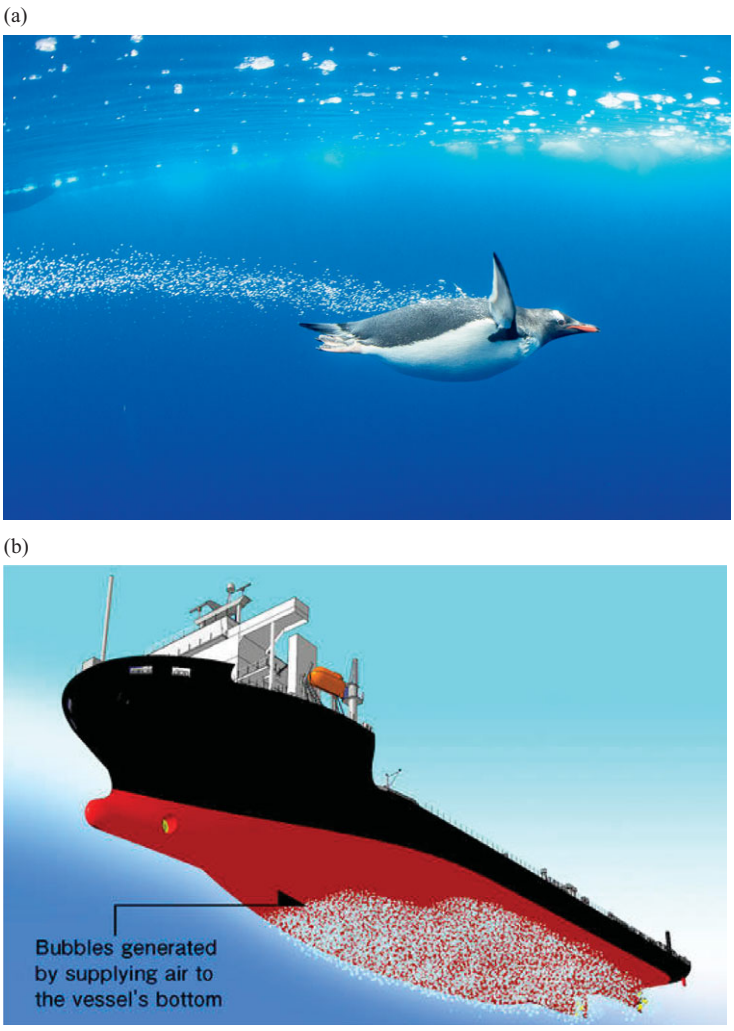

Figure 1.12 Drag reduction using bubbly flow: (a) emperor penguins releasing bubbles from their feathers to reduce hydrodynamic drag (Nolan, 2018); and (b) concept design of microbubbles injected along a ship hull to reduce drag (Kaisha, 2010).

especially if near a constriction or turn. Plaque deposits can be especially dangerous if they break off from a vessel wall and move downstream as an agglomeration (a collection of many smaller accreted particles). This larger particle can be transported downstream to a smaller blood vessel, where it can lodge itself and obstruct the blood flow. If this happens in a brain blood vessel, the blockage may lead to a stroke.

An example of a biomedical system with multiphase air flow is an inhaler, which rapidly delivers a medicinal aerosol spray to the respiratory system (Figure 1.15a). The fine aerosol droplets are intended to evaporate as they reach the lungs. Some of the droplets will instead deposit on mucous surfaces along the complex flow path

https://doi.org/10.1017/9781139028806.002 Published online by Cambridge University Press

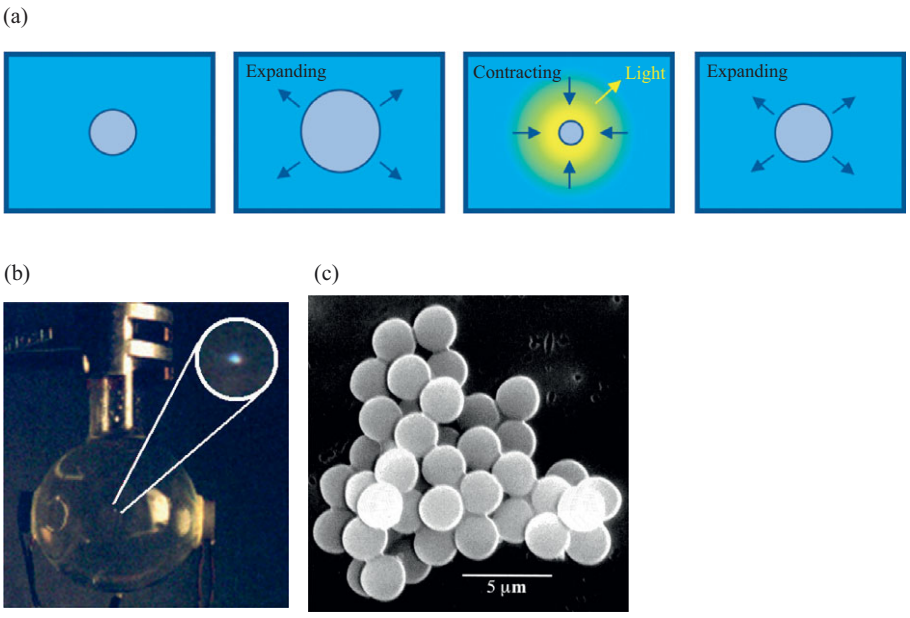

Figure 1.13 Sonoluminescence of microbubbles: (a) diagram of the contraction–expansion process whereby the maximum contraction causes very high pressures and temperatures, yielding light emission; (b) experimental setup to excited microbubble volume dynamics (Geisler, 1999); and (c) protein microspheres produced by this process (Suslick and Price, 1999).

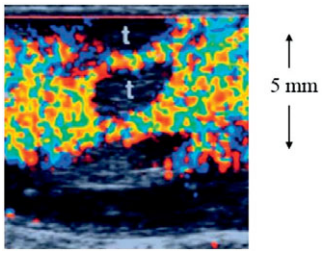

Figure 1.14 Ultrasonic Doppler image of a rabbit liver injected with microbubbles (about 3 μm in diameter) showing acoustic emission signals from the bubbles as colored regions where lack of signals can allow tumor regions to be detected, as marked with "t" (Forsberg et al., 1999).

through the mouth and throat. The deposition mechanism depends on particle size, as it is generally driven by particle inertia and gravity for drops with diameters greater than 1 μm but by stochastic Brownian motion for drop diameters of 0.1 μm or less. As a result of deposition and evaporation, the average drop size changes along the pathway from the mouth to the lungs (Figure 1.15b). One must account for these factors to predict the overall effectiveness of aerosol drug delivery.

However, some airborne droplets are harmful, as they can carry diseases such as the Covid virus. These droplets can be dispersed via breathing, but especially by sneezing and

https://doi.org/10.1017/9781139028806.002 Published online by Cambridge University Press

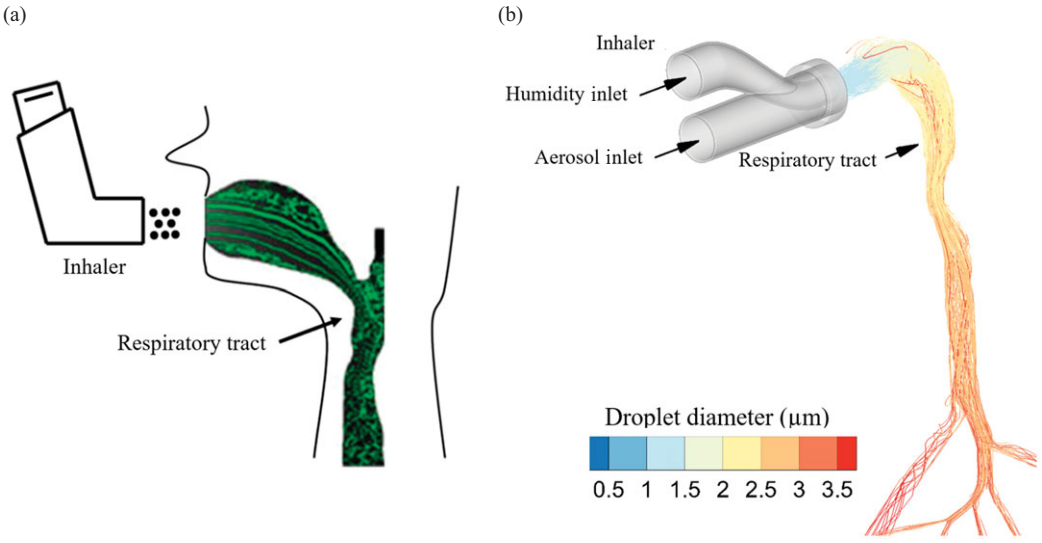

Figure 1.15 Aerosol droplet trajectories: (a) in the simulated geometry of an upper respiratory tract (mouth and throat) to study inhaler aerosol delivery effectiveness (based on a figure by Niven et al., 1994); and (b) change in droplet sizes as the trajectories move to the lungs (Longest, 2019).

Figure 1.16 Aerosol droplets resulting from a human cough can travel significant distances (Butler, 2020).

coughing (Figure 1.16). The larger droplets can have significant inertia, leading to longer distances of travel, and therefore a facial mask or covering can be crucial to help prevent breathing in these droplets. Breathing in solid particles in the air can also be unhealthy. These airborne particles can stem from atmospheric pollution caused by both man-made and natural systems. Our respiratory pathway employs mucous deposition so that most particles don't reach the lungs, where they can do damage to the sensitive lung tissue.

https://doi.org/10.1017/9781139028806.002 Published online by Cambridge University Press

(a)

AQI	AQI category	$PM_{2.5}$ ($\mu g/m^3$)	PM_{10} ($\mu g/m^3$)
0–50	Good	0–15	0–54
51–100	Moderate	16–40	55–154
101–200	Unhealthy	41–150	155–254
201–300	Very unhealthy	151–250	255–354
301 or more	Hazardous	251 or more	355 or more

(b)

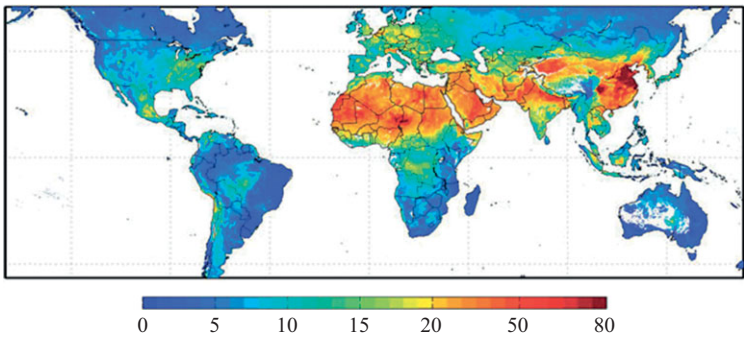

(c)

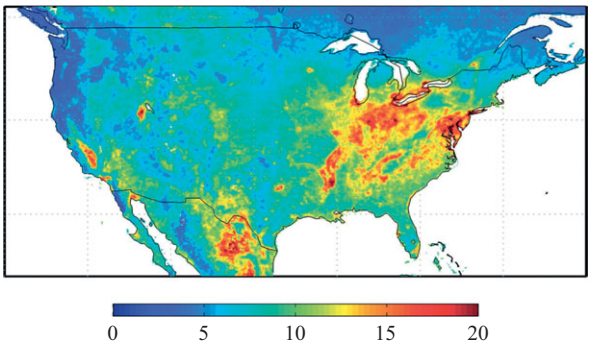

Figure 1.17 Atmospheric particle concentration: (a) Air Quality Index (AQI) as a function of particle matter (PM) concentration and size, where PM_{10} and $PM_{2.5}$ are respectively based on particle diameters of 10 μm or less and based on 2.5 μm or less; (b) global and (c) North American distribution of $PM_{2.5}$ in levels of $\mu g/m^3$ (van Donkelaar, 2010).

Because of the potential harm of solid particles to human and other animal respiratory systems, the distribution of these particles in the near-surface atmosphere is of special interest. To help assess the potential health impact of airborne particles, a standardized Air Quality Index (AQI) was established by the United States Environmental Protection Agency based on $PM_{2.5}$ and PM_{10}, defined respectively as concentration of particle matter with diameters of 2.5 and 10 μm or less (Figure 1.17a). However, these distributions can be difficult to predict and to control since particle concentrations are influenced by natural environments and human activities that vary

https://doi.org/10.1017/9781139028806.002 Published online by Cambridge University Press

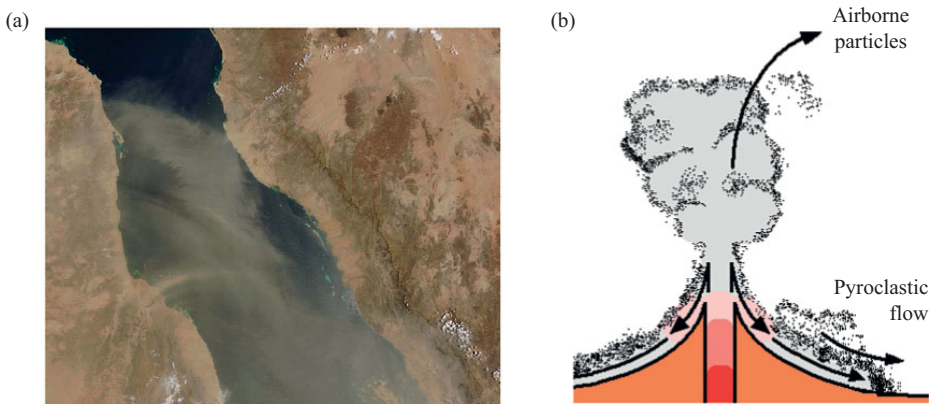

Figure 1.18 Natural events that cause air-laden multiphase flow: (a) atmospheric spread of particles over the Red Sea region by a dust storm (Ahmadi, 2005); and (b) volcanic-induced particle ejection whereby most particles are ejected into the atmosphere, but high-concentration ash-laden pyroclastic flows can also be driven downward.

widely with time and location. For example, the world's highest $PM_{2.5}$ concentrations (Figure 1.17a) tend to be in arid regions and deserts, such as northern Africa, where there are high concentrations of surface particles (e.g., sand) that can be lifted into the air, and there is little ground vegetation to help capture and filter such airborne particles. In addition, regions with heavy transportation, manufacturing, construction, and carbon-based energy production also lead to high $PM_{2.5}$ concentrations, such as regions in the US below the Great Lakes and in the Mid-Atlantic (Figure 1.17b). Furthermore, topography can play an important role for localized regions. For example, weather inversions in low-level areas surrounded by mountain can lead to smog (fog or haze combined with smoke and other atmospheric pollutants) that can persist for long periods. Recently, the PM_1 concentrations (based on particle diameters of 1.0 μm or less) has raised concern since these nanoparticles can more easily reach the lungs and may be medically harmful (though there is not enough understanding to implement within the AQI).

In addition, the transport of larger atmospheric particles is also important since these are more likely to impact natural habitats, surface vegetation, etc. Particles injected into the atmosphere from forest fires or dust storms can be carried hundreds of miles (Figure 1.18a). Volcanic eruptions can also create airborne particles (Figure 1.18b), which can distribute fine ash on a continental scale. Figure 1.18b shows that volcanos can also create *pyroclastic* flows, whereby high particle concentrations create a high mixture density that moves downward along the surface of the volcano and then spreads radially outward. These pyroclastic flows (driven by changes in density) can be particularly dangerous due to their near-zero oxygen content, high temperatures (up to 600°C), fast speeds (up to 100 km/hr), and large ranges (they can travel as far as 60 km). In fact, pyroclastic flows are the main cause of human death from volcanic events (Chester, 1993). The airborne ash can curtail airplane flight

https://doi.org/10.1017/9781139028806.002 Published online by Cambridge University Press

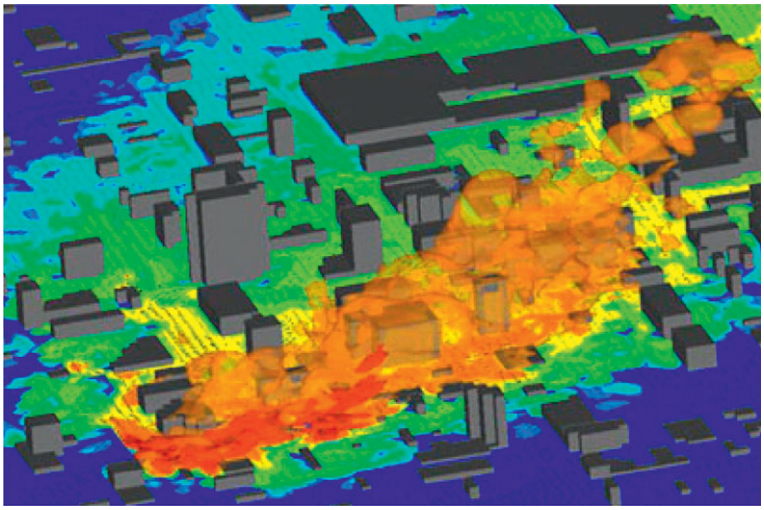

Figure 1.19 Simulated wind-driven dispersal of hazardous airborne particles in an urban area (DeCroix, 2003).

paths in the short term as well as also impact agriculture and surface water quality in the long term. Hazardous airborne particles can also be created when there are fires at chemical or manufacturing facilities. Another concern is the nefarious release of dangerous particles in highly populated urban areas where wind flow interacting with buildings dictates localized dispersal (Figure 1.19).

The transport of sediment in natural bodies of water can also be a concern. The settling and suspension transport is governed by turbulence, topology, and weather events, all of which can be problematic. For example, high sedimentation can reduce river capacity, leading to flooding that negatively impacts agricultural and/or populated regions. On the other hand, erosion of rivers and coastal areas can cause loss of animal habitats and natural hurricane barriers.

In some cases, water streams contain man-made solid particles from manufacturing or waste treatment plants. Such particles should be removed but are difficult to settle, as they are nearly buoyant. One removal method employs floatation though bubble attachment. In this three-phase flow process, microbubbles are added to the solid unwanted matter (Figure 1.20a), so it is carried upward through flotation and then skimmed off before it can proceed downstream (Figure 1.20b).

Transport of bubbles in natural bodies of water is also important to the environment. For example, carbon dioxide and methane bubbles released from ocean beds influence the temperature, salinity, and acidity of the ocean water. Another example is the man-made introduction of bubble plumes into freshwater reservoirs and other nearly static water bodies. The turbulent mixing by these plumes can increase oxygen content and control pH levels to improve the overall ecological health of these freshwater bodies.

Bubble plumes have even been used by humpback whales and dolphins to create "bubble nets," as shown in Figure 1.21. In particular, the animals dive below and then

https://doi.org/10.1017/9781139028806.002 Published online by Cambridge University Press

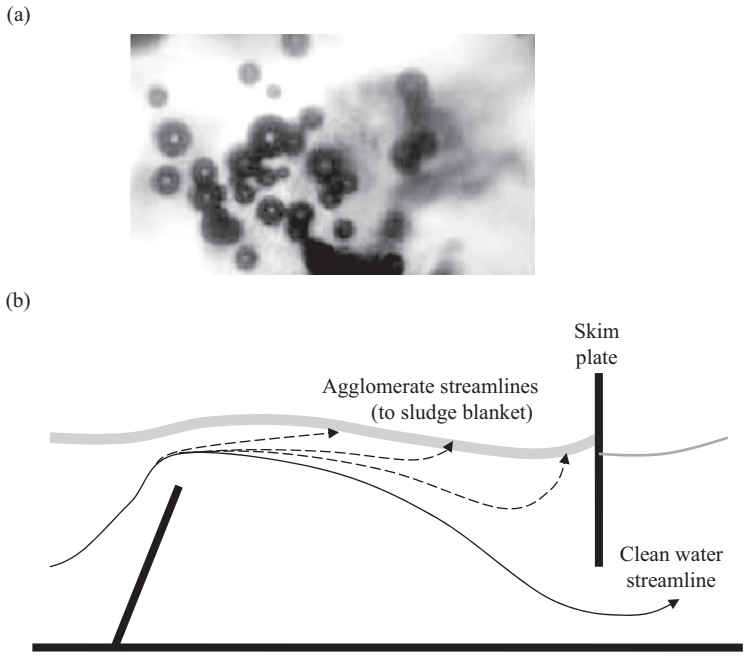

Figure 1.20 Particles filtered from a water stream by attaching small bubbles (ranging from 30–300 μm) to cause unwanted particle matter to float to the surface for skimming. (a) An image of a buoyant agglomeration consisting of microbubbles (dark spheres) attached to a single loosely aggregated flocculation particle (large gray shape) in order to cause enhanced flotation (Leppinen and Dalziel, 2004). (b) Schematic of a water stream with path lines of buoyant agglomerates (particles surrounded by microbubbles) filtered to the surface while clean water passes underneath the skimmer.

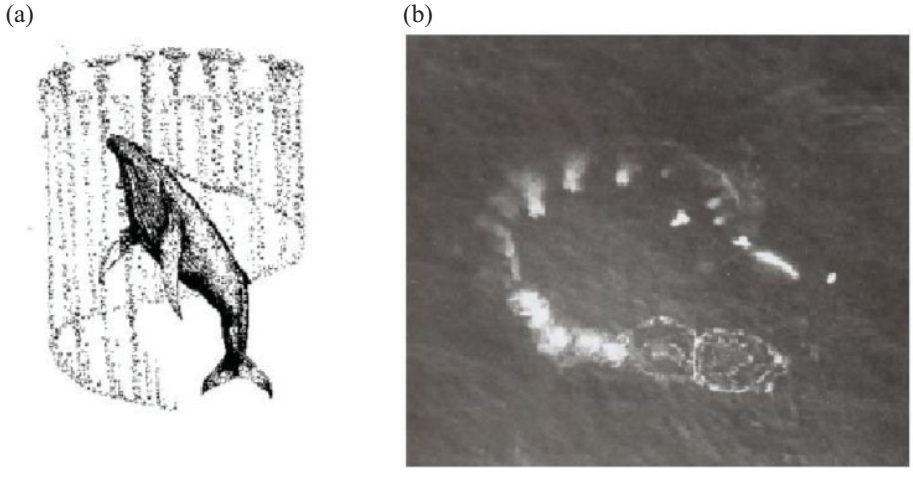

Figure 1.21 A humpback whale making a bubble net using its blowhole: (a) schematic of the bubble release along a helical path; and (b) surface photograph of bubbles reaching the surface (Leighton, 2004).

https://doi.org/10.1017/9781139028806.002 Published online by Cambridge University Press

exhale air through their blowholes as they spiral upward to create a cylindrical wall of bubbles. This bubble wall temporarily "traps" the prey, allowing the predator to feed more easily.

1.3 Basic Terminology and Assumptions for Particle Fluid Dynamics

1.3.1 Basic Multiphase Definitions

A few essential definitions will be introduced to describe the basic features of a dispersed multiphase flow. First, a *particle* is defined as an unattached, freely moving body immersed in a fluid, which is the *surrounding flow*. The particle phase may be a solid, a liquid (i.e., drop), or a gas (i.e., bubble), while the surrounding fluid can be a gas or a liquid. This text specifically focuses on dispersed flow for which particle motion is primarily influenced by that of the surrounding flow rather than by particle collisions. Such flows are called *dilute*. In contrast, *dense flow* occurs when particle collisions dominate particle motion, which is more likely at high particle concentrations. Recommended texts that focus on dense flows are noted in the preface.

For dispersed flow, the collection of all the particles in the flow domain is defined as the *dispersed phase*, while the surrounding fluid is defined as the *continuous phase*. The latter definition assumes that the surrounding flow can be considered as a continuum (an assumption discussed further in §1.5). Thus, a two-phase dispersed flow has a single dispersed phase of particles and a single continuous phase of fluid. However, this concept can be extended to three phases (e.g., a continuous-phase liquid flow that includes both bubbles and solid particles as the dispersed phases).

Dispersed flow can also include the special case of two immiscible liquids, that is, two fluids separated by surface tension and are insoluble (no molecular mixing) so that each fluid's properties (density, viscosity, etc.) remain distinct. For example, oil drops in water generally have a preserved interface between the two liquids. As a result, the dynamics of such oil drops in water are similar to that of solid particles with the same density and size. Notably, this special case only applies to liquids since gases are miscible with other gases.

1.3.2 Basic Particle Nomenclature

In this section, the key variables for the basic properties of a particle (dispersed phase) and the surrounding fluid (continuous phase) are defined. These (and all other variables and symbols used in this text) are listed in the "Nomenclature" section near the beginning of this book.

To generalize the notation, we first define subscripts for the phases. The continuous-phase variables and properties will be designated by the subscript f (e.g., ρ_f is the surrounding fluid's density and μ_f is its dynamic viscosity), while the dispersed-phase variables and properties will be typically designated by the subscript p (e.g., ρ_p is the particle density). For a fluid particle (i.e., a drop or a bubble), one may

https://doi.org/10.1017/9781139028806.002 Published online by Cambridge University Press

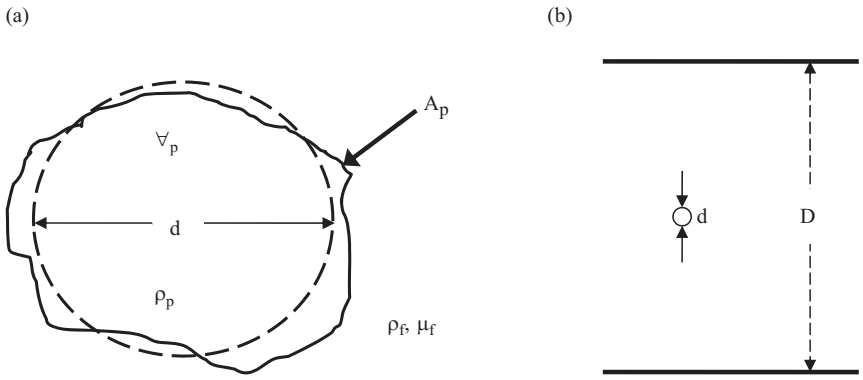

Figure 1.22 Schematic of (a) a nonspherical particle (solid line) with given volume and surface area surrounded by a continuous-phase fluid density and viscosity, along with the equivalent-volume sphere (dashed line), and (b) a particle that is small compared to a channel width, such that d « D.

define the internal particle viscosity as μ_p (Figure 1.22a). In addition, we designate a gas or a liquid property with the respective subscripts g and ℓ.

In terms of geometry, the particle volume is $\forall_p$ and its surface area is A_p. For an arbitrary shape (Figure 1.22a), we then define the *volumetric diameter* d as the diameter of a sphere that has the same volume as that of the particle, as follows:

$$\forall_p = \pi d^3/6 \qquad \textit{for a sphere with a diameter } d. \tag{1.1a}$$

$$d \equiv 2r_p \equiv \left(6\forall_p/\pi\right)^{1/3} \qquad \textit{for spherical or nonspherical shape}. \tag{1.1b}$$

Note that the use of $\equiv$ denotes the definition of a variable (not just an equality) and that (1.1b) defines the volumetric radius $\left(r_p\right)$ as equal to half the volumetric diameter. If the particle is a sphere, its radius and diameter are equal to the volumetric radius and diameter. If the particle is not a sphere, the particle surface area will always be larger than the surface area of a spherical particle that has the same volume, as follows:

$$A_p \geq A_{p,\text{sphere}} = 4\pi r_p^2 = \pi d^2. \tag{1.2}$$

The extent of this inequality increases as the particle shape deviation (from a sphere) increases.

For dispersed flow (the focus of this text), the particle is assumed to be much smaller than the macroscopic length scale of the continuous-flow domain, which is defined as D. This assumption can be expressed as

$$d \ll D. \tag{1.3}$$

Note that D may represent the diameter of a pipe (as in Figure 1.22b), the width of a jet, or another key macroscopic length scale of the flow domain.

https://doi.org/10.1017/9781139028806.002 Published online by Cambridge University Press

Next we consider ratios of the density and viscosity. The particle density (ρ_p) is defined as the ratio of particle mass (m_p) to particle volume:

$$\rho_p \equiv m_p/\forall_p. \tag{1.4}$$

This density relative to that of the fluid (ρ_f) is important for many multiphase flows. For example, the *specific gravity* is the ratio of the particle density to the water density. As such, a particle will float or sink in water depending on whether the specific gravity is less than or greater than unity.

To make a more general comparison for any surrounding fluid density, the particle density ratio is defined as

$$\rho_p^* \equiv \rho_p/\rho_f. \tag{1.5}$$

In this text, a * superscript is used to indicate a dimensionless version of a variable. Similarly, a fluid particle will have a particle viscosity and a surrounding fluid viscosity that can be used to define the particle viscosity ratio as

$$\mu_p^* \equiv \mu_p/\mu_f. \tag{1.6}$$

These ratios for density and viscosity will be shown later to influence particle dynamics, and the limits for very small and very large ratios are often important.

To consider such limits, a set of key comparison symbols is defined for a dimensionless quantity (using the example variable q) as follows:

$$q \to 0 \text{ } \textit{indicates} \text{ q } \textit{is very small (e.g., < 0.01 or less) and may be neglected.} \tag{1.7a}$$

$$q \ll 1 \quad \textit{indicates} \text{ q } \textit{is small (e.g., } \sim \textit{0.1 or less) but is considered finite.} \tag{1.7b}$$

$$q \tilde{<} 1 \quad \textit{indicates} \text{ q } \textit{is typically less than unity.} \tag{1.7c}$$

$$q \sim 1 \quad \textit{indicates} \text{ q } \textit{is of the order unity.} \tag{1.7d}$$

$$q \gtrsim 1 \quad \textit{indicates} \text{ q } \textit{is typically more than unity.} \tag{1.7e}$$

$$q \gg 1 \quad \textit{indicates} \text{ q } \textit{is large (e.g., 10 or more).} \tag{1.7f}$$

$$q \to \infty \quad \textit{indicates} \text{ q } \textit{is very large (e.g., 100 or more).} \tag{1.7g}$$

For example, solid and liquid densities are generally much greater than gas densities, so liquid drops and solid particles in a gas can be characterized by $\rho_p \gg \rho_f$. Such particles are defined as *high-density* particles. In contrast, gas bubbles in a liquid with $\rho_p \ll \rho_f$ are defined *high-buoyancy* particles. Particles with intermediate densities with $\rho_p \sim \rho_f$ (e.g., solid particles with a specific gravity near unity in water) are defined as *near-neutrally buoyant*. If the particle and the surrounding are both fluids, the viscosity ratio can also be defined. Since liquid viscosities are generally much greater than gas viscosities, a drop in a gas corresponds to $\mu_p \gg \mu_f$, while a gas bubble corresponds to $\mu_p \ll \mu_f$.

https://doi.org/10.1017/9781139028806.002 Published online by Cambridge University Press

1.3.3 Vector Notation

In the next section, two types of multiphase velocities are defined. These will employ both vectors and scalars. Herein, a vector (e.g., force, velocity, etc.) is represented by **boldface** (e.g., $\mathbf{q}$), while the scalar magnitude of a vector (a positive value) is represented by a regular typeface (e.g., $q = |\mathbf{q}|$).

Cartesian vector components can be defined using subscripts for the x-, y-, and z-directions or using index notation in the 1, 2, and 3 directions. For example, an arbitrary vector $\mathbf{q}$ can be expressed using x, y, and z and 1, 2, and 3 subscripts as

$$\mathbf{q} \equiv q_x\mathbf{i}_x + q_y\mathbf{i}_y + q_z\mathbf{i}_z = q_1\mathbf{i}_1 + q_2\mathbf{i}_2 + q_3\mathbf{i}_3 = q_i\mathbf{i}_i \qquad (1.8a)$$

$$q \equiv |\mathbf{q}| = \sqrt{q_x^2 + q_y^2 + q_z^2} = \sqrt{q_i q_i} \qquad \textit{for } i = 1, 2, \textit{and } 3. \qquad (1.8b)$$

The double appearance of the subscript i in the right-hand side (RHS) product indicates a tensor summation operation over all the index values (i = 1, 2, and 3). In this text, this notation will be generally used whenever index summation is intended (otherwise, summation is not intended). The position vector $\mathbf{X}$ is also useful to consider reference frames and is defined based on a position relative to reference point. Following (1.8), it can be expressed in terms of Cartesian components as

$$\mathbf{X} \equiv x\mathbf{i}_x + y\mathbf{i}_y + z\mathbf{i}_z = X_1\mathbf{i}_1 + X_2\mathbf{i}_2 + X_3\mathbf{i}_3 = X_i\mathbf{i}_i \qquad \textit{for } i = 1, 2, \textit{and } 3. \qquad (1.9)$$

For a Cartesian coordinate system, the divergence of a vector $\mathbf{q}$ (with components q_x, q_y, and q_z) and the gradient of a scalar q can be expressed in coordinate notation or tensor notation (using the position vector components) as follows:

$$\nabla \cdot \mathbf{q} \equiv \frac{\partial q_x}{\partial x} + \frac{\partial q_y}{\partial y} + \frac{\partial q_z}{\partial z} = \frac{\partial q_1}{\partial X_1} + \frac{\partial q_2}{\partial X_2} + \frac{\partial q_3}{\partial X_3} \equiv \frac{\partial q_i}{\partial X_i}. \qquad (1.10a)$$

$$\nabla q \equiv \frac{\partial q}{\partial x}\mathbf{i}_x + \frac{\partial q}{\partial y}\mathbf{i}_y + \frac{\partial q}{\partial z}\mathbf{i}_z = \frac{\partial q}{\partial X_1}\mathbf{i}_1 + \frac{\partial q}{\partial X_2}\mathbf{i}_2 + \frac{\partial q}{\partial X_3}\mathbf{i}_3 \equiv \frac{\partial q}{\partial X_i}\mathbf{i}_i. \qquad (1.10b)$$

The left-hand side (LHS) and RHS provide compact forms for divergence of a vector and gradient of a scaler.

For a spherical coordinate system, the coordinates in the radial, polar, and azimuthal direction are r, θ, and ϕ directions as shown in Figure 1.23. As such, a velocity vector $\mathbf{q}$ can be expressed in terms of the components q_r, q_θ, and q_ϕ. In this case, the divergence and gradient for a spherical reference frame can be expressed as

$$\nabla \cdot \mathbf{q} = \frac{1}{r^2}\frac{\partial(r^2 q_r)}{\partial r} + \frac{1}{r\sin\theta}\frac{\partial(q_\theta \sin\theta)}{\partial\theta} + \frac{1}{r\sin\theta}\frac{\partial\left(q_\phi\right)}{\partial\phi}. \qquad (1.11a)$$

$$\nabla q \equiv \frac{\partial q}{\partial r}\mathbf{i}_r + \frac{1}{r}\frac{\partial q}{\partial\theta}\mathbf{i}_\theta + \frac{1}{r\sin\theta}\frac{\partial q}{\partial\phi}\mathbf{i}_\phi. \qquad (1.11b)$$

https://doi.org/10.1017/9781139028806.002 Published online by Cambridge University Press

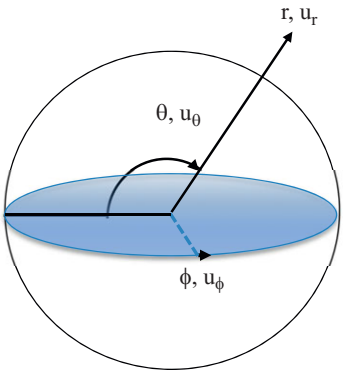

Figure 1.23 Spherical coordinate system for a velocity $\mathbf{u}$, where r is the radial coordinate and u_r is the radial velocity component (both in the direction of unit vector $\mathbf{i}_r$), where θ is the polar angle and u_θ is the polar velocity component, and where ϕ is the azimuthal angle about the axis $\theta = 0$ and u_ϕ is the azimuthal velocity component.

This coordinate system is often useful for considering flow around a particle, as will be shown in Chapter 3. For this, azimuthal symmetry will be generally assumed for the flow, which indicates there is no dependence on ϕ and u_ϕ is zero.

1.4 Resolved-Surface and Point-Force Velocity Fields

The velocity fields for multiphase flow are generally categorized as (1) *resolved-surface* velocities, which consider how the flow moves locally around the particle surface; or (2) *point-force* velocities, which neglect the particle surface and instead consider motion based on the particle centroid. These two flow fields are quite different (the first is based on physical geometry, and the second is based on theoretical approximation), but each will be used at different times throughout the book. In the following subsections, these two categories of velocity fields are first discussed individually and then they are compared.

1.4.1 Resolved-Surface Velocity Fields

The resolved-surface velocity fields are defined relative to a particle surface whose interface locations are defined by $\mathbf{X}_I$, as shown in Figure 1.24, where the subscript I indicates the particle surface interface. Relative to this interface, the continuous-phase velocity field outside of the particle surface is denoted by $\mathbf{U}$. For this surrounding flow, each point on the surface $(\mathbf{X}_I)$ can experience viscous and pressure stresses. The combination of these stresses integrated over the particle surface determines the net fluid dynamic forces acting on a particle. The pressure stresses on the particle are based on P_f and only contribute toward the surface normal direction. As will be discussed in Chapter 2, the viscous stresses are based on the velocity field

https://doi.org/10.1017/9781139028806.002 Published online by Cambridge University Press

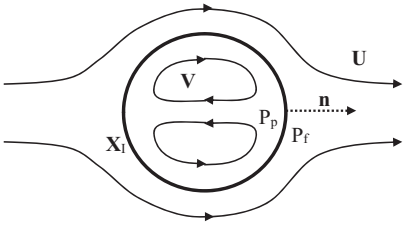

Figure 1.24 Schematic of fluid particle cross-section interface (thick solid line) whose points have coordinates $\mathbf{X}_I$ and whose outward normal is $\mathbf{n}$, which separates the two resolved-surface velocity and pressure fields, given as $\mathbf{U}$ and P_f for the external surrounding fluid and given as $\mathbf{V}$ and P_p for the internal particle fluid.

gradients and the surrounding fluid viscosity. If the particle is a solid, P_f is often simplified as P.

If the particle is a fluid, there can also be an internal flow defined by $\mathbf{V}$ (as shown in Figure 1.24). Note that $\mathbf{U}$ and $\mathbf{V}$ take into account the local geometry of the particle surface, which need not be spherical. Thus, the two resolved-surface velocity fields and pressure fields for a fluid particle are given as follows:

$$\mathbf{U} \equiv \text{continuous-phase velocity external to the particle surface.} \tag{1.12a}$$

$$P_f \equiv \text{continuous-phase pressure external to the particle surface.} \tag{1.12b}$$

$$\mathbf{V} \equiv \text{dispersed-phase velocity within the particle surface.} \tag{1.12c}$$

$$P_p \equiv \text{dispersed-phase pressure within the particle surface.} \tag{1.12d}$$

The internal velocity field will create internal viscous stresses (based on μ_p) and a field of internal pressure (P_p). There will be a jump condition between P_f and P_p at the interface due to surface tension and surface curvature. Formulations for these internal fluid stresses and the pressure jump for a particle will be discussed in Chapter 3.

If there is no mass transfer across the interface, the normal components of $\mathbf{U}$ and $\mathbf{V}$ will be equal at the interface surface. If one further assumes a continuum surrounding flow with finite viscosity (see §1.5), the tangential components of $\mathbf{U}$ and $\mathbf{V}$ must also be equal at the interface $(\mathbf{X}_I)$. Therefore, there is no jump in the velocity at the interface, as follows:

$$\mathbf{U}_I = \mathbf{V}_I \text{ at } \mathbf{X}_I \quad \textit{for continuum flow with no mass transfer.} \tag{1.13}$$

This is often described as the "no-slip" condition. If the particle's shape and size are also fixed in time, the external and internal flow field streamlines associated with $\mathbf{U}$ and $\mathbf{V}$ will follow along the particle surface geometry (as shown in Figure 1.24).

1.4.2 Point-Force Velocities

In many cases, only the net fluid dynamic force on the particle is of interest (not the details of the local fluid and particle velocity fields near the interface). In such a case,

https://doi.org/10.1017/9781139028806.002 Published online by Cambridge University Press

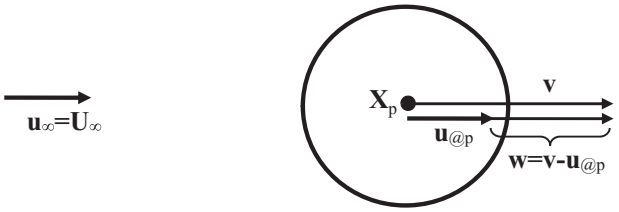

Figure 1.25 Point-force velocity schematics for a nonspinning solid particle with centroid-based velocity ($\mathbf{v}$) exposed to a spatially uniform, unhindered, continuous-phase velocity ($\mathbf{u}_\infty$), creating a relative velocity ($\mathbf{w}$) based on the difference when extrapolated to the particle centroid ($\mathbf{u}_{@p}$).

this net force can be assumed to act at a single point located at the centroid of the particle, that is, as a *point force*. The corresponding point-force velocities are also based on the particle centroid $(\mathbf{X}_p)$, as illustrated in Figure 1.25. In particular, the translational velocity $(\mathbf{v})$ is the particle centroid velocity, which can vary with time (t) along the particle path. The particle's translational velocity and centroid position vectors can be expressed using the Cartesian unit vectors of (1.9), as follows:

$$\mathbf{v}(t) \equiv v_x(t)\mathbf{i}_x + v_y(t)\mathbf{i}_y + v_z(t)\mathbf{i}_z. \tag{1.14a}$$

$$\mathbf{X}_p(t) \equiv x_p(t)\mathbf{i}_x + y_p(t)\mathbf{i}_y + z_p(t)\mathbf{i}_z. \tag{1.14b}$$

Since these are referenced to the centroid, these are particle Lagrangian reference frame values.

Next we define the velocity of surrounding fluid in the point-force reference frame $(\mathbf{u})$ as the fluid velocity that neglects the presence and motion of the particle. Thus, the flow defined by $\mathbf{u}$ is "unhindered" by the particle. In particular, $\mathbf{u}$ ignores the local details of the flow path deflection around the particle surface or any other aspect of the particle's presence (and is thus nonphysical). Note that if there are other particles in the domain, $\mathbf{u}$ takes into account their integrated influence on the flow but not the influence of the particle for which it is being referenced.

If one interpolates the unhindered surrounding velocity field $(\mathbf{u})$ to the particle centroid $(\mathbf{X}_p)$, this is termed the surrounding fluid velocity "seen" by the particle and is denoted as $\mathbf{u}_{@p}$. This hypothetical velocity allows one to define a relative particle velocity $(\mathbf{w})$ as the difference between the particle and that of the unhindered surrounding fluid, so that $\mathbf{w} = \mathbf{v} - \mathbf{u}_{@p}$. This relative velocity can be related to various net fluid dynamic forces acting on the particle. For example, the drag force will be found to act in the direction of $-\mathbf{w}$ (drag resists relative velocity motion), and the drag magnitude increases as the relative velocity magnitude increases.

Similarly, the pressure of the unhindered surrounding fluid (which ignores the particle's presence) can be interpolated to the particle centroid as $p_{f@p}$. The definitions for the preceding velocities and this pressure field can be summarized as follows:

https://doi.org/10.1017/9781139028806.002 Published online by Cambridge University Press

$$\mathbf{v} \equiv \text{translation velocity of particle centroid} \equiv \left.\frac{\mathbf{X}_p(t+\Delta t)-\mathbf{X}_p(t)}{\Delta t}\right|_{\Delta t\to 0}. \quad (1.15a)$$

$$\mathbf{u} \equiv \text{surrounding fluid velocity unhindered by the particle's presence.} \quad (1.15b)$$

$$\mathbf{u}_{@p}(t) \equiv \mathbf{u}\left(\mathbf{X}_p, t\right) \equiv \text{unhindered flow velocity interpolated to } \mathbf{X}_p. \quad (1.15c)$$

$$\mathbf{w}(t) \equiv \mathbf{v}(t) - \mathbf{u}_{@p}(t) \equiv \text{particle relative velocity to the unhindered flow.} \quad (1.15d)$$

$$p \equiv \text{continuous-phase pressure neglecting local particle disturbances.} \quad (1.15e)$$

It is important to note that $\mathbf{u}_{@p}$ is hypothetical since the particle does indeed affect the surrounding fluid and since the surrounding fluid does not exist at the centroid (inside the particle). However, $\mathbf{u}_{@p}$ is mathematically and computationally convenient since it defines a local relative velocity that is proportional to drag, lift, and other fluid dynamic particle forces.

The preceding point-force approach can be similarly applied to other properties. Particle rotation about the centroid can be characterized by angular velocity $\left(\boldsymbol{\Omega}_p\right)$, and the unhindered surrounding fluid vorticity (which ignores the particle's presence) can be interpolated to the particle centroid as $\omega_{f@p}$. Particle temperature can be characterized by a single temperature (T_p), which reflects the integrated temperature within the particle volume, and the unhindered surrounding fluid temperature can be interpolated to the particle centroid as $T_{f@p}$.

1.4.3 Contrasting Point-Force and Resolved-Surface Velocities

The point-force and resolved-surface velocity fields are contrasted in Figure 1.26, where the surrounding point-force flow field $\mathbf{u}$ is independent of the particle presence (Figure 1.26a), while the resolved surrounding velocity $\mathbf{U}$ around the particle (Figure 1.26b) has increased complexity. In addition, the resolved continuous-fluid velocity $(\mathbf{U})$ is only defined outside the particle interface, while $\mathbf{u}_{@p}$ is defined at the

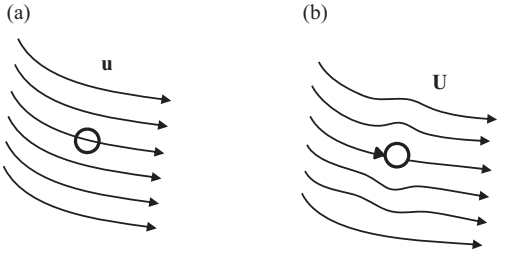

Figure 1.26 Comparing streamlines for different representations of the surrounding velocity field for a stationary particle ($\mathbf{v} = 0$), showing (a) the unhindered flow field ($\mathbf{u}$), which extends hypothetically to the particle centroid where it produces a relative velocity at the centroid, that is, $\mathbf{v} \neq \mathbf{u}$ at $\mathbf{X}_p$, and (b) the resolved-surface flow around same particle showing that $\mathbf{U}$ deviates around the particle surface and matches the surface velocity, that is, $\mathbf{U} = \mathbf{V}$ at $\mathbf{X}_I$.

https://doi.org/10.1017/9781139028806.002 Published online by Cambridge University Press

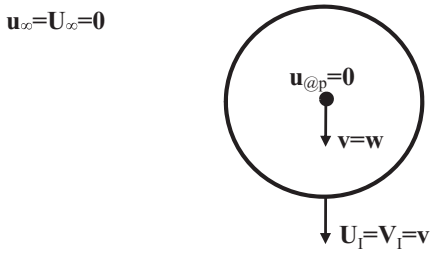

Figure 1.27 A solid nonspinning particle falling in a still fluid. The resolved-surface and point-force surrounding fluid velocities are both far from the particle, but the resolved-surface value tends to the particle velocity as it approaches a point on the particle surface (due to the no-slip condition). The point-force surrounding fluid velocity remains zero up to and even inside the particle.

particle centroid. Furthermore, the point-force velocity fields define a relative velocity of the particle to surrounding fluid (1.15d), while there is no relative velocity between the phases for the resolved-surface fields (1.13).

To further compare the point-force and resolved-surface velocities, consider the simplified case where the particle is solid and not spinning, so $\mathbf{V}$ becomes a constant within the interface. As such, all parts of the particle move at the centroid velocity, that is, $\mathbf{v} = \mathbf{V}$. If we further assume the surrounding fluid is a constant value and steady far from the particle, this far-field velocity is the same for both reference frames, that is, $\mathbf{u}_\infty = \mathbf{U}_\infty$. However, as we get closer to the particle interface, the velocity fields of $\mathbf{u}$ and $\mathbf{U}$ differ, since $\mathbf{u}$ will stay a constant, but $\mathbf{U}$ will be altered by the presence of the particle. For example, consider a particle falling at velocity $\mathbf{v}$ in a large quiescent tank so $\mathbf{u}_\infty = \mathbf{U}_\infty = \mathbf{0}$ as in Figure 1.27. However, the surrounding fluid near the particle will be affected by the local pressure and shear stresses associated with the particle movement. For finite viscosity, the no-slip condition of (1.13) dictates $\mathbf{U}_I = \mathbf{V}_I = \mathbf{v}$. In contrast, the unhindered velocity neglects the presence of the particle motion, including at the centroid, so $\mathbf{u}_{@p} = 0$. As such, $\mathbf{U} \neq \mathbf{u} = \mathbf{0}$ in the vicinity of the particle, and the particle's relative translational velocity in this stagnant medium is given by $\mathbf{w} = \mathbf{v}$.

If one considers multiple particles in a domain, it should be noted that $\mathbf{u}_{@p}$ for a given particle only neglects the flow disturbances associated with the particle at $\mathbf{X}_p$. However, the $\mathbf{u}$ velocity field generally can be modified by the combined point forces associated with all other particles in the domain. For example, if we consider a large number of particles falling in one portion of an otherwise static fluid, the downward momentum induced by the falling particles will lead to a regional downdraft of the fluid so $\mathbf{u} \neq 0$. In this way, $\mathbf{u}_{@p}$ incorporates the net downdraft induced by all the other particles.

1.4.4 Point-Force Time Derivatives

Since flow and particle properties can vary in space $(\mathbf{x})$ and in time (t), it is important to properly define their rate of change with regard to a specific reference frame. The temporal variation can be based on three reference frames, as shown in Figure 1.28:

https://doi.org/10.1017/9781139028806.002 Published online by Cambridge University Press

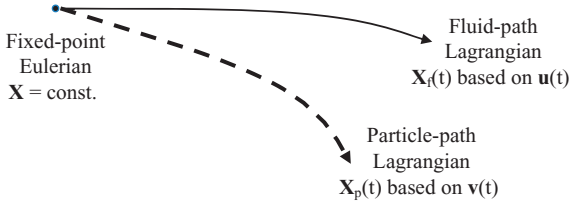

Figure 1.28 Schematic showing the three reference frames based on an Eulerian point ($\mathbf{X}$ = constant), a Lagrangian-particle path (based on $\mathbf{X}_p$ and $\mathbf{v}$ as a function of time) and Lagrangian-fluid path (based on $\mathbf{X}_f$ and $\mathbf{u}$ as a function of time). The particle and fluid element paths differ since the particle is also falling downward.

- Eulerian, referenced to a fixed point in space
- Particle-Lagrangian, referenced to the particle centroid and its velocity $\mathbf{v}$
- Fluid-Lagrangian, referenced to the fluid path and its velocity $\mathbf{u}$

Note that the Lagrangian derivative is also sometimes called the material derivative, as it follows a specific material (the fluid or the particle).

To compare the three reference frames, consider the analogy of a bridge over a river with a duck. The Eulerian reference frame is effectively the stationary (no velocity) vantage point at the bridge. The fluid-Lagrangian reference frame is the vantage of a fluid element (a tracer), which moves exactly with the stream's speed and direction (e.g., a small leaf on the river surface). The particle-Lagrangian reference frame is the vantage of the duck, whose motion is influenced by the river flow but can have a distinct trajectory as it paddles, since the duck velocity ($\mathbf{v}$) will not generally equal the river velocity ($\mathbf{u}$). So the amount and direction of paddling by the duck will dictate its relative velocity ($\mathbf{w}$).

The time derivatives for each of these reference frames are expressed in the following equation using an arbitrary scalar q. The Eulerian time derivative is based on temporal changes at a fixed point within the domain.

$$\frac{\partial q}{\partial t} \equiv \left.\frac{q(\mathbf{X}, t + \Delta t) - q(\mathbf{X}, t)}{\Delta t}\right|_{\Delta t \to 0}. \tag{1.16}$$

In contrast, the particle-Lagrangian and fluid-Lagrangian time derivatives are respectively defined along the particle path (defined with by $\mathbf{v}$) and the fluid path (defined with $\mathbf{u}$) as:

$$\frac{\mathcal{d}q}{\mathcal{d}t} \equiv \left.\frac{q(\mathbf{X} + \mathbf{v}\Delta t, t + \Delta t) - q(\mathbf{X}, t)}{\Delta t}\right|_{\Delta t \to 0} = \frac{\partial q}{\partial t} + \mathbf{v} \cdot \nabla q. \tag{1.17a}$$

$$\frac{\mathcal{D}q}{\mathcal{D}t} \equiv \left.\frac{q(\mathbf{X} + \mathbf{u}\Delta t, t + \Delta t) - q(\mathbf{X}, t)}{\Delta t}\right|_{\Delta t \to 0} = \frac{\partial q}{\partial t} + \mathbf{u} \cdot \nabla q. \tag{1.17b}$$

These RHS expressions make use of the chain rule and the notation of (1.10b) while assuming that the scalar field is continuously differentiable in space. The two LHS derivatives can be related using the relative velocity of (1.15d) as follows:

https://doi.org/10.1017/9781139028806.002 Published online by Cambridge University Press

$$\frac{d'q}{d't} = \frac{\mathcal{D}q}{\mathcal{D}t} + \mathbf{v}\cdot\nabla q - \mathbf{u}\cdot\nabla q = \frac{\mathcal{D}q}{\mathcal{D}t} + \mathbf{w}\cdot\nabla q. \tag{1.18}$$

Referring to our previous river analogy, time changes seen in a Eulerian frame would be like those seen looking straight down from the bridge, where one may observe a floating leaf appear from under the bridge that would then float downstream out of one's field of view. Time changes seen in a particle-Lagrangian frame would be like those seen by the duck, which may observe different small leaves on the river surface due to its relative velocity.

Next we consider the time derivatives for a vector (that varies continuously in space). The changes in the vector as seen by a particle-Lagrangian reference frame can be related to the Eulerian and fluid-Lagrangian time derivatives in vector form $(\mathbf{q})$ and in Cartesian tensor form (q_i) as follows:

$$\frac{d'\mathbf{q}}{d't} = \frac{\partial \mathbf{q}}{\partial t} + (\mathbf{v}\cdot\nabla)\mathbf{q} = \frac{\partial \mathbf{q}}{\partial t} + (\mathbf{u}\cdot\nabla)\mathbf{q} + (\mathbf{w}\cdot\nabla)\mathbf{q} = \frac{\mathcal{D}\mathbf{q}}{\mathcal{D}t} + (\mathbf{w}\cdot\nabla)\mathbf{q}. \tag{1.19a}$$

$$\frac{d'q_i}{d't} = \frac{\partial q_i}{\partial t} + v_j\frac{\partial q_i}{\partial X_j} = \frac{\partial q_i}{\partial t} + u_j\frac{\partial q_i}{\partial X_j} + w_j\frac{\partial q_i}{\partial X_j} = \frac{\mathcal{D}q_i}{\mathcal{D}t} + w_j\frac{\partial q_i}{\partial X_j} \; for \; j = 1,2,3. \tag{1.19b}$$

Note that a key assumption in applying the preceding derivative relations to a flow property is that that the property (density, velocity field, etc.) continuously varies in space.

1.5 Continuum Criteria and Conditions

1.5.1 Normal Temperature and Pressure

A helpful reference condition for properties of a given fluid is Normal Temperature and Pressure (NTP), which is defined by a reference (room) temperature and pressure: $T_{ref} = 293\ K$ and $p_{ref} = 101,320\ N/m^2$. NTP properties are given in Table A.1 for two gases (air and methane) and two liquids (water and ethanol).

1.5.2 Continuum Criteria

This text generally assumes a "continuum" approximation for the surrounding fluid. In this limit, the drag on a body will be shown to be a function of pressure and viscosity (Chapter 3). This is true if the fluid properties are based on bulk averages of a large number of molecular interactions. However, this assumption is not appropriate if one considers flow length scales similar to the molecular scales on the surrounding fluid.

To clarify the difference between continuum and noncontinuum conditions, consider a particle surrounded by gas molecules (Figure 1.29). If we consider individual molecules, their collisions with the particle surface will be stochastic and discrete. Since these collisions determine the fluid influence on the particle at any given time,

https://doi.org/10.1017/9781139028806.002 Published online by Cambridge University Press

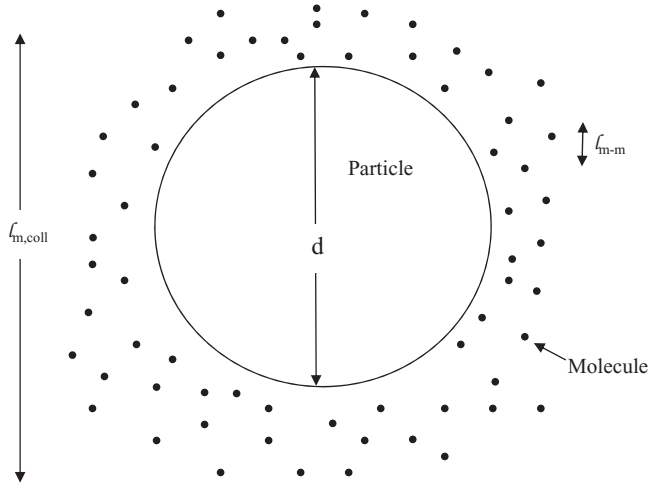

Figure 1.29 Schematic of molecules (small solid spheres) of a surrounding gas near a small particle (e.g., 10 nanometers). The length-scale criterion for density and temperature is based on the molecular spacing ($\ell_{m\text{-}m}$), while the criterion for continuum pressure and viscosity is based on the mean free path between molecular collisions ($\ell_{m,coll}$) where $\ell_{m,coll} \gg \ell_{m\text{-}m}$.

the influence of the fluid will also be stochastic and discrete. If we instead consider continuum conditions, the number of molecular interactions (averaged in both time and space) is large enough such that their integrated influence becomes deterministic and continuous. The net fluid influence can then be expressed in terms of pressure and fluid stresses on the surface. For the example of a fixed particle in a static fluid, the pressure at the continuum scale is a constant while the influence at the molecular scale is based on the individual molecular impacts. In the following, the criterion for continuum conditions is characterized in terms of length scales for a gas and is then considered more generally for a liquid as the surrounding fluid.

For a gas that makes up the surrounding fluid, there are three key length scales associated with the molecules as shown in Figure 1.29:

- The effective diameter of a molecule (d_m), based on its cross-sectional area
- The average spacing between molecules $(\ell_{m\text{-}m})$, which determines the gas density once combined with the molecular mass
- The average distance that a molecule will travel before hitting another molecule $(\ell_{m,coll})$, termed the molecular mean free

Continuum conditions for particles are typically defined in terms of the fluid stresses (since these determine the forces on the particle) and thus require $d \gg \ell_{m,coll}$. To quantify this effect, the particle Knudsen number (Kn_p) is defined as the ratio of the molecular mean free path length to the particle diameter:

$$Kn_p \equiv \frac{\ell_{m,coll}}{d}. \tag{1.20}$$

https://doi.org/10.1017/9781139028806.002 Published online by Cambridge University Press

This ratio can be used to set a criterion for continuum conditions, as follows:

$$\mathrm{Kn_p} \to 0 \qquad \textit{Gas flow around the particle is a continuum.} \tag{1.21}$$

Thus, a very small $\mathrm{Kn_p}$ corresponds to a statistically large number of molecular collisions distributed over the particle surface to ensure that the pressure and viscous stress fields are in continua (i.e., both are smoothly varying in space) and are not a function of the Knudsen number. To illustrate the latter assumption, the particle drag for a sphere at $\mathrm{Kn_p} = 0.01$ is about 98% of the drag at $\mathrm{Kn_p} \to 0$ (where the latter is only a function of viscosity and pressure). As such, $\mathrm{Kn_p} < 0.01$ is often used as a reasonable approximation for (1.21).

Notably, for a gas at typical atmospheric conditions, the average spacing between molecules is typically 10–20 times the size of molecules (such that $\ell_{\mathrm{m-m}} \gg \mathrm{d_m}$), while the mean free path is about 30 times larger than the spacing between molecules (such that $\ell_{\mathrm{m,coll}} \gg \ell_{\mathrm{m\text{-}m}}$). This latter difference is illustrated in Figure 1.29, where the molecular spacing is small relative to the particle size (indicating the particle is nearly large enough for the surrounding gas density to be considered as a continuum). However, the mean free path is larger than the particle diameter (indicating that this corresponds to strongly noncontinuum conditions). As such, the continuum conditions based on pressure and viscous stresses (1.21) are even more stringent than those based on density (and temperature).

To consider the continuum assumption for a single-phase flow, one may similarly define a fluid domain-scale Knudsen number in terms of the fluid domain length scale (D of 1.3), as follows:

$$\mathrm{Kn_D} \equiv \frac{\ell_{\mathrm{m,coll}}}{\mathrm{D}}. \tag{1.22}$$

This length scale ratio can be similarly used to set a continuum criterion for single-phase flow, as follows:

$$\mathrm{Kn_D} \to 0 \qquad \textit{Gas flow acts as a continuum at the domain length scales.} \tag{1.23}$$

Since the particle diameters herein are assumed to be much smaller than that of the fluid domain (per 1.3), it follows that $\mathrm{Kn_D} \ll \mathrm{Kn_p}$. Therefore, if continuum conditions are reasonable for flow around the particle, they will automatically also be reasonable for the overall flow field.

To compute the Knudsen number for a particular gas, we first define an *ideal gas* as having the following relationship among pressure, temperature, density, and the specific gas constant $\left(\mathcal{R}_g\right)$:

$$\mathrm{p}_g = \rho_g \mathcal{R}_g \mathrm{T}_g. \tag{1.24a}$$

$$\mathcal{R}_g \equiv \mathcal{R}_{\mathrm{univ}}/\mathrm{MW}_g. \tag{1.24b}$$

The latter equation employs the universal gas constant, $\mathcal{R}_{\mathrm{univ}} = 8314.47\mathrm{J}/(\mathrm{kmol\text{-}K})$ and the molecular weight of the gas $\left(\mathrm{MW}_g\right)$. Next we employ the hard sphere model for the molecules (Hirschfelder et al., 1954), so that the mean free path is related to the fluid

https://doi.org/10.1017/9781139028806.002 Published online by Cambridge University Press

viscosity (based on the mean molecular collision cross section), the gas density (based on the molecular spacing), and the mean relative molecular velocity magnitude ($v_{m\text{-}m}$, based on the average speed of molecules they approach each another), as follows:

$$\ell_{m,coll} = \frac{2\mu_g}{\rho_g v_{m\text{-}m}} = \frac{\mu_g}{\rho_g} \frac{\sqrt{\pi}}{\sqrt{2\mathcal{R}_g T_g}} \qquad \textit{for an ideal gas.} \tag{1.25a}$$

$$v_{m\text{-}m}^2 = 8\mathcal{R}_g T_g/\pi \tag{1.25b}$$

The expression of (1.25b) relates the mean relative kinetic energy of the molecules to the gas temperature (T_g) and the gas constant. While the expression of (1.25a) can be used with (1.20) to determine if the continuum approximation is reasonable for a flow about a particle. For example, the mean free path for air (based on Table A.1 properties) yields $\ell_{m,coll}$ of about 0.07 μm. If one applies a continuum criterion of $Kn_p < 0.01$, this requires $d > 7\,\mu m$ for the flow about the particle. As such, smaller particles (or lower gas densities, e.g., at a high altitude) may result in significant noncontinuum effects.

For a liquid, the continuum criteria based on pressure and viscous stresses are not as well defined. This is because the molecules are more tightly spaced and tend to interact continuously, such that a mean free path description is not appropriate. However, the mean molecular spacing $(\ell_{m\text{-}m})$ is still relevant to define fluid density. For typical liquids, this spacing is less than a nanometer, so that density can be considered a continuum for particle diameters as small as 100 nanometers. This continuum criterion $(d > 100\ell_{m\text{-}m})$ can also be applied for the effects of pressure and viscosity for liquids, that is, the average drag of a particle is unaffected by molecular spacing for this condition.

While these length-scale criteria can be used to determine continuum conditions in an averaged sense, random molecular effects can also be considered in an unsteady sense. In particular, discrete molecular collisions can cause particles as large as 1 μm (in a liquid or a gas) to move irregularly due to Brownian motion. This effect requires an analysis based on kinetic theory (instead of length scales), as will be discussed in §5.3. In addition, Knudsen number effects for a particle in a gas are discussed in §9.2.2–9.2.3. Otherwise, the rest of this text will assume continuum conditions for flow around the particle and for the flow in the domain.

1.6 Chapter 1 Problems

(P1.1) With 100–150 words and one or two figures, identify and discuss an engineering or environmental system that involves a dispersed multiphase flow with solid particles, drops, and/or bubbles that was not presented with a figure in §1.2. Focus your discussion on the importance of this flow system, the relevant multiphase interaction physics, and any research issues. To support the latter, cite two archival research references that are relevant to this flow.

https://doi.org/10.1017/9781139028806.002 Published online by Cambridge University Press

(P1.2) Consider a wind tunnel where the flow is steady and is moving in the positive x-direction (left to right) through a contraction. The unhindered air speed variation with downstream distance for $x > 0$ is given as $u_o(1 + x/L)^{1/2}$, where $u_o = 0.25\,m/s$ and $L = 0.4\,m$. Consider a solid nonrotating particle that is also moving left to right in this flow, but its inertia causes its centroid to move at a nearly fixed speed of 0.24 m/s along the tunnel centerline. When the particle is at $x/L = 0.5$, determine (a) $\mathbf{U}, \mathbf{V}$, and $d\mathbf{U}/dt$ on the particle surface as well as (b) $\mathbf{u}_{@p}, \mathbf{w}, d\mathbf{v}/dt$, and $\mathcal{D}\mathbf{u}/\mathcal{D}t$.

(P1.3) A tank of water that sloshes back at forth with a spatially uniform cyclic velocity given by $u = u_D \sin(2\pi t/\tau_D)$, where u_D is the peak velocity magnitude and is given by 0.5 m/s, while τ_D is the oscillation period and is given by 1.5 s. In this flow, consider a neutrally buoyant particle whose centroid has a cyclic velocity given by $v = v_D \sin(2\pi t/\tau_D)$, where $v_D = 0.5u_D$ due to particle inertia (ignoring phase lag). At $t = 0.5$ s, determine the time-varying (a) $\mathbf{U}, \mathbf{V}$, and $d\mathbf{U}/dt$ on the particle surface as well as (b) $\mathbf{u}_{@p}, \mathbf{w}, d\mathbf{v}/dt$, and $\mathcal{D}\mathbf{u}/\mathcal{D}t$.

(P1.4) For an altitude of 10 km (where $p = 26,400$ Pa, $T = -50°C$, and $\mu_f = 1.447 \times 10^{-5}$ kg/m-sec), determine the minimum diameter of a particle for which the surrounding air can considered to be in continuum conditions.

https://doi.org/10.1017/9781139028806.002 Published online by Cambridge University Press